© 2020. Published by The Company of Biologists Ltd | Journal of Cell Science (2020) 133, jcs241034. doi:10.1242/jcs.241034

RESEARCH ARTICLE

RGS4 controls Gαi3-mediated regulation of Bcl-2 phosphorylation on TGN38-containing intracellular membranes

Guillaume Bastin[1,2,3,‡], Kaveesh Dissanayake[3,*], Dylan Langburt[1,3,*], Alex L. C. Tam[3], Shin-Haw Lee[1,3], Karanjit Lachhar[3] and Scott P. Heximer[1,2,3]

ABSTRACT

Intracellular pools of the heterotrimeric G-protein α-subunit Gαi3 (encoded by *GNAI3*) have been shown to promote growth factor signaling, while at the same time inhibiting the activation of JNK and autophagic signaling following nutrient starvation. The precise molecular mechanisms linking Gαi3 to both stress and growth factor signaling remain poorly understood. Importantly, JNK-mediated phosphorylation of Bcl-2 was previously found to activate autophagic signaling following nutrient deprivation. Our data shows that activated Gαi3 decreases Bcl-2 phosphorylation, whereas inhibitors of Gαi3, such as RGS4 and AGS3 (also known as GPSM1), markedly increase the levels of phosphorylated Bcl-2. Manipulation of the palmitoylation status and intracellular localization of RGS4 suggests that Gαi3 modulates phosphorylated Bcl-2 levels and autophagic signaling from discreet TGN38 (also known as TGOLN2)-labeled vesicle pools. Consistent with an important role for these molecules in normal tissue responses to nutrient deprivation, increased Gαi signaling within nutrient-starved adrenal glands from RGS4-knockout mice resulted in a dramatic abrogation of autophagic flux, compared to wild-type tissues. Together, these data suggest that the activity of Gαi3 and RGS4 from discreet TGN38-labeled vesicle pools are critical regulators of autophagic signaling that act via their ability to modulate phosphorylation of Bcl-2.

KEY WORDS: Gαi3, RGS4, Bcl-2, DHHC, Palmitoylation, Autophagy

INTRODUCTION

Heterotrimeric G-proteins mediate the effects of hormones and neurotransmitters that signal via G-protein coupled receptors (GPCRs) at the plasma membrane (Hepler and Gilman, 1992; Sánchez-fernández et al., 2014). In its quiescent state, the GDP-bound Gα subunit is bound to a Gβγ heterodimer. GPCR activation leads to exchange of GTP for GDP on the α-subunit, resulting in the dissociation of Gα and Gβγ subunits and initiation of downstream effector signaling pathways. The signal is terminated following hydrolysis of GTP to GDP by the intrinsic GTPase activity of the Gα subunit, and the system returns to its inactive state. Recent studies, however, have shown that some α subunits are localized to intracellular membrane compartments such as the trans-Golgi network (TGN) (Almeida et al., 1993; Wylie et al., 1999; Lo et al., 2015; Hewavitharana and Wedegaertner, 2012; Michaelson et al., 2002; Nash et al., 2019), endoplasmic reticulum-Golgi intermediate compartment (ERGIC) (Le-niculescu et al., 2005; Lo et al., 2015), multivesicular bodies (MVBs) (Zheng et al., 2004; Rosciglione et al., 2014) or the nucleus where they exert novel (Willard and Crouch, 2000; Hewavitharana and Wedegaertner, 2012; Vaniotis et al., 2011; Tadevosyan et al., 2012), albeit less well understood, signaling functions. Indeed, Gαi3 (encoded by *GNAI3*) has been found both at the plasma membrane and within several intracellular compartments where it has been shown to regulate cellular functions such as membrane trafficking (Wilson et al., 1993; Lo et al., 2015), cell migration (Ghosh et al., 2008), macrophage polarization (Li et al., 2015) and autophagy (macroautophagy) in response to nutrient deprivation (Ogier-denis et al., 1996; Gohla et al., 2007; Pattingre et al., 2003; Ghosh et al., 2008). Notably, most of the mechanisms that mediate the activation of intracellular Gαi3 and its functional role in these pathways remain to be determined.

Accordingly, many studies have been aimed at understanding regulatory proteins for Gαi3 that modulate its activity on intracellular membranes in a GPCR-independent manner. Cytosolic guanine nucleotide exchange factors (GEFs) such as GIV (also known as Girdin or CCDC88A) bind to α-subunits to promote GDP release, GTP-binding and Gαi3 activation (Le-niculescu et al., 2005; Garcia-marcos et al., 2011). By contrast, guanine nucleotide dissociation inhibitors (GDIs), such as AGS3 (also known as GPSM1), maintain the GDP-bound inactive state of the α subunit (Pattingre et al., 2003; Garcia-marcos et al., 2011) and regulator of G-protein signaling (RGS) proteins catalyze the intrinsic GTPase activity of α subunits, leading to rapid and potent inhibition of activated Gαi signals (Watson et al., 1996; Berman et al., 1996a,b). One such protein, RGS4, has been shown to traffic between the plasma membrane and intracellular (TGN38-marked) membrane pools, where differential palmitoylation of N-terminal cysteine residues (Cys2 and Cys12) have been shown to be key determinants in its ability to localize to TGN38 (also known as TGOLN2) endomembranes and to regulate intracellular Gαi3 (Bastin et al., 2012, 2015). Using RGS4 trafficking mutants as membrane pool-specific inhibitors, we have previously shown that Gαi3 localized to intracellular membranes where, in its activated state, it diminished the activation of intracellular pools of the stress kinase, JNK (also known as MAPK8) (Bastin et al., 2015). Other groups have shown that JNK-mediated phosphorylation of Bcl-2 has important functional consequences for the regulation of its structure and function (Yamamoto et al., 1999; Wei et al., 2008; Pattingre et al., 2009). Specifically, they showed JNK could initiate phosphorylation of multiple residues within the flexible loop

[1]Ted Rogers Centre for Heart Research, Translational Biology and Engineering Program, 661 University Ave. 14th Floor, Toronto, ON, M5G 1M1, Canada. [2]Heart and Stroke/Richard Lewar Centre of Excellence in Cardiovascular Research, Room 303, C. David Naylor Building, 6 Queen's Park Crescent West, Toronto, ON, M5S 3H2, Canada. [3]Department of Physiology, University of Toronto, 1 King's College Circle, Toronto, ON, M5S1A8, Canada.
*These authors contributed equally to this work

‡Author for correspondence (guillaume.bastin@univ-lorraine.fr)

G.B., 0000-0001-8422-2564; D.L., 0000-0002-5924-0442; K.L., 0000-0001-6079-4525

Handling Editor: John Heath
Received 30 October 2019; Accepted 5 May 2020

Journal of Cell Science (2020) 133, jcs241034. doi:10.1242/jcs.241034

domain in Bcl-2 following microtubule inhibition (G2/M arrest) or nutrient deprivation (Yamamoto et al., 1999). As a result, JNK-mediated phosphorylation of Bcl-2 resulted in changes in its function as a regulator of autophagy and apoptosis in response to stress stimuli (Yamamoto et al., 1999; Wei et al., 2008; Pattingre et al., 2009). Using cell biological tools to control distinct intracellular pools of RGS4 and Gαi3, we here set out to determine whether their intracellular activity could regulate Bcl-2 phosphorylation and whether these proteins function under nutrient-deprived conditions in cultured HEK293 cells.

RESULTS

Gαi3 activity reduces the phosphorylation of Bcl-2

To examine the role of Gαi3 activity in HEK293 cells, a Gαi3-knockout (KO) cell line was generated using a CRISPR/Cas9 gene-editing strategy (see Materials and Methods and Fig. S1). HEK293 cells transfected with Bcl-2 and different activity-state constructs of Gαi3 were cultured under nutrient-deprived conditions to examine whether Gαi3 activity regulated stress kinase and Bcl-2 activity. Expression of constitutively active Gαi3 (Gαi3-RC) caused a greater inhibition of intracellular JNK phosphorylation (activation) than expression of the wild-type Gαi3 construct (Bastin et al., 2015). Importantly, the decrease in JNK activity was also associated with a marked decrease in the levels of Ser70 phosphorylated Bcl-2 (P-Bcl-2) (Fig. 1A). Together, these data suggest that under conditions of cellular stress, activated (GTP-bound) Gαi3 reduces the phosphorylation of Bcl-2 via its ability to inhibit the stress-induced kinase JNK.

RGS4 increases Bcl-2 phosphorylation mediated by Gαi3

Co-expression of wild-type RGS4 (WT), a potent Gαi3 inhibitor, increased the level of P-Bcl-2 compared to a catalytically dead RGS4 (EN-AA) isoform (Fig. 1B). The effect of RGS4 was greatest when it was co-expressed with the GAP-sensitive (Berman et al., 1996a) constitutively-active Gαi3-RC construct (Coleman et al., 1994), consistent with the notion that either the activity state (i.e. GTP- or GDP-bound) or GTPase cycling function of Gαi3 is an important regulator of P-Bcl-2 levels in our system. Expression of AGS3, an inhibitor of Gαi3 activation that has been shown to be localized to ER and Golgi membranes (Oner et al., 2013), also promoted increased levels of P-Bcl-2 to the same extent as RGS4 (Fig. S2). Moreover, the P-Bcl-2-elevating effects of RGS4 could be prevented by either mutation of the RGS domain to the Gαq-selective 'triple-mutant' (RGS4-3x) form or by co-expression of a RGS-insensitive mutant of Gαi3 (Gαi3-GS; Fig. S2). Surprisingly, P-Bcl-2 levels were not increased when RGS4 was co-expressed with a non-cycling GAP-resistant (Berman et al., 1996a,b) constitutively active mutant of Gαi3, Gαi3-QL (Coleman et al., 1994; Sondek et al., 1994) (Fig. 1C). Since RGS proteins form stable complexes with Gα-QL isoforms (presumably GTP-bound) in mammalian expression systems, we conclude that either (1) the P-Bcl-2 inhibiting effects of GTP-bound Gαi3 are not affected by RGS4 binding; or (2) Gαi3 cycling between GTP- and GDP-bound states is required for its regulation of this pathway.

DHHC3 and DHHC7 facilitate intracellular RGS4 trafficking via palmitoylation of its N-terminal cysteine residues

While RGS4 localizes to both plasma membrane and intracellular membrane pools, it is the intracellular pool that modulates Gαi3 and JNK activity during nutrient deprivation (Bastin et al., 2015). We asked whether factors that control the ability of RGS4 to traffic via different membrane pools might therefore influence the extent of Bcl-2 phosphorylation. Differential palmitoylation of Cys2 and Cys12 in RGS4 regulates its ability to traffic between different membrane pools, but the molecular mechanisms that control this trafficking are not well understood (Bastin et al., 2012). Wang and colleagues have shown that two palmitoyl-CoA transferases, DHHC3 and DHHC7, are important for the palmitoylation and function of RGS4 to inhibit GPCR signaling at the plasma membrane (Wang et al., 2010). Amidst the 23 known DHHC isoforms (also known as ZDHHC isoforms) in humans (Fukata et al., 2006; Ohno et al., 2006), mRNAs for *DHHC3* and *DHHC7* were among the most highly expressed in our HEK293 cells (Fig. 2; Table S1). Other highly expressed isoforms include *DHHC5*, *DHHC18* and *DHHC21*. While previous studies suggest a similar Golgi localization pattern for DHHC3 and DHHC7 (Ohno et al.,

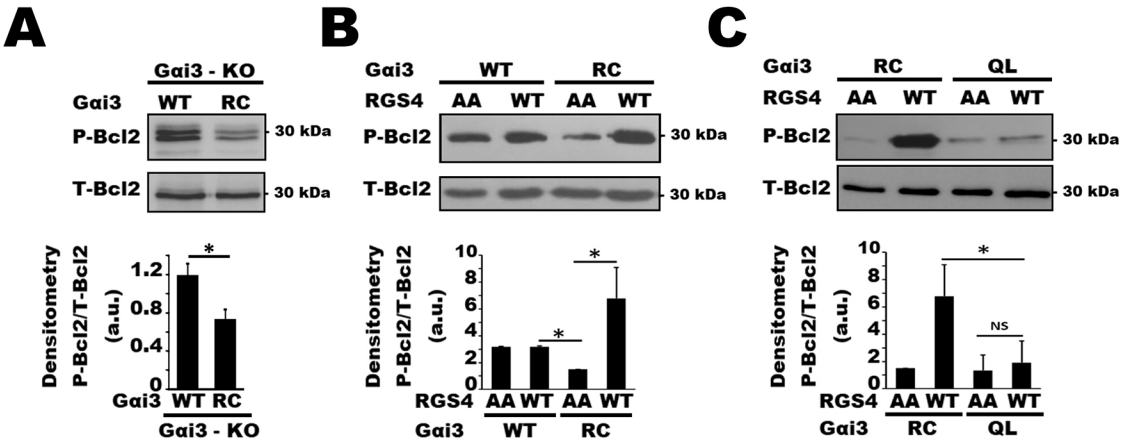

Fig. 1. RGS4 and Gαi3 coordinately regulate phosphorylation of Bcl-2 on Ser70 under nutrient-deprived conditions. (A) Western blots (upper panel) for phospho (P)-Bcl-2 and total (T)-Bcl-2 levels in CRISPR-Gαi3-KO HEK293 cells transiently expressing either a WT or RC allele of Gαi3. Histogram (lower panel) shows the mean±s.e.m. quantification of the P-Bcl-2:T-Bcl-2 ratios. (B,C) Wild-type (WT) and an inactive RGS4 (ENAA) mutant were tested for their ability to modulate Gαi3-mediated reduction of P-Bcl-2 levels. (B) Examines the effects of RGS4 activity on WT Gαi3 and a GTPase-capable constitutively active isoform Gαi3 (RC). (C) Examines the effects of RGS4 activity on Gαi3(RC) and a GTPase-defective constitutively active isoform Gαi3(QL). The upper panel(s) show western blots for P-Bcl-2 and T-Bcl-2, while the lower panels contain the mean±s.e.m. quantification of P-Bcl-2:T-Bcl-2 ratios, as in A. In all panels, data are representative of at least three independent experiments carried out on separate days (n=3). *P<0.05; NS, not significant [unpaired t-test (A), two-way ANOVA and Tukey's post-hoc test (B,C)]. a.u., arbitrary units.

Journal of Cell Science (2020) 133, jcs241034. doi:10.1242/jcs.241034

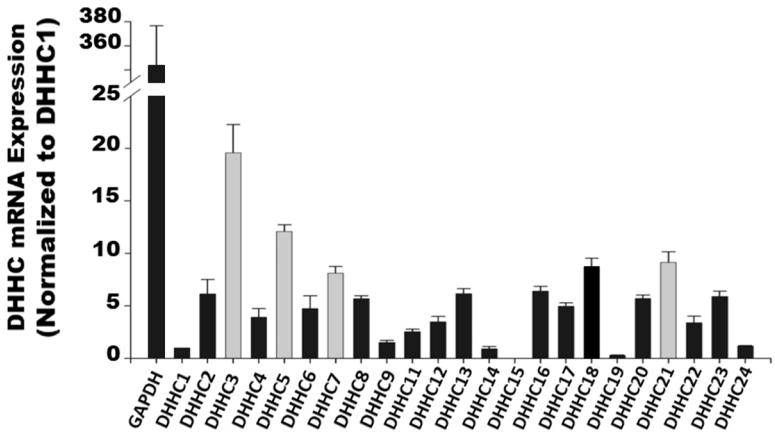

Fig. 2. Levels of endogenous mRNA expression of DHHC proteins in HEK293 cells. The level of expression of DHHC mRNAs were determined by RT-qPCR. CT data are normalized to DHHC1 and for reference purposes shown relative to GAPDH. The levels of expression of DHHC 3, 5, 7 and 21 are highlighted by gray colors. Error bars represent s.e.m. (*n*=3). The data are the means of three independent experiments carried out on separate days.

2006), careful examination shows that these two proteins have overlapping, but distinct, expression patterns in HEK293 cells (Fig. S3). HA-tagged DHHC3 targeted large perinuclear bodies resembling the Golgi, whereas HA-tagged DHHC7 was found in both Golgi-like structures and endosome-like membranes scattered throughout the cell (Fig. S3). Co-expression of either HA–DHHC3 or HA–DHHC7 with their putative substrate, RGS4-YFP, induced redistribution of the RGS4 localization pattern to resemble that of each DHHC isoform (Figs S4, S5) (Ohno et al., 2006). Such strong accumulation of RGS4 (also called 'substrate trapping') has been used to indicate DHHC–substrate interactions for a number of different DHHCs (Fukata et al., 2004; Huang et al., 2004). Notably, co-expression of DHHC5 and DHHC21 with RGS4 did not result in a similar substrate-trapping phenotype. To confirm that Cys2 and Cys12 in RGS4 were the primary targets of DHHC3 and DHHC7 in HEK293 cells, we co-expressed alanine mutations of these constructs with both DHHCs. As expected Cys2 and Cys12 mutation dramatically reduced the amount of RGS4 that accumulated on intracellular membranes when co-expressed with DHHC3 or DHHC7 (Fig. 3A,B).

DHHC3 and DHHC7 differentially regulate RGS4 intracellular membrane targeting

Using dominant-negative DHHC mutants (denoted DHHS), we next asked whether the endogenous DHHC3 and DHHC7 affected the ability of RGS4 to traffic between the plasma membrane, the Golgi, and endosomal vesicles where Gαi3 is also known to localize and function. Expression of both DHHS3 and DHHS7 reduced the amount of RGS4 at the plasma membrane and increased its accumulation in intracellular membrane pools (Fig. 4A–C; Fig. S5), consistent with our previous data (Bastin et al., 2012), showing that palmitoylation was required for proper intracellular trafficking of RGS4. siRNA-mediated knockdown of DHHC3 and DHHC7 produced similar results (Fig. S6). Inhibition of DHHC7 with DHHS7, decreased the colocalization of RGS4–YFP with TGN38–cerulean-marked vesicles as indicated by a decrease in the Pearson correlation coefficient (PCC) from 0.48 to 0.15 (Fig. 5A,B). DHHS7 expression not only decreased the proportion of endosomes in which RGS4 colocalized with TGN38, it also directed RGS4 to smaller-sized endosomes within the cell (Fig. 5C). By contrast, DHHC3 inhibition by DHHS3 did not affect RGS4–TGN38 colocalization coefficients, the proportion of endosomes showing colocalization or the size of RGS4-containing endosomes (Fig. 5A–C). Together, these data indicate that DHHC3 and DHHC7 have distinct functions with respect to directing the intracellular trafficking and function of RGS4 on intracellular membrane pools.

Bcl-2 phosphorylation is regulated by Gαi3 and RGS4 from within discreet TGN38-marked compartments

When the effect of DHHC3 and DHHC7 inhibition were examined for their relative ability to modulate the function of RGS4 to inhibit

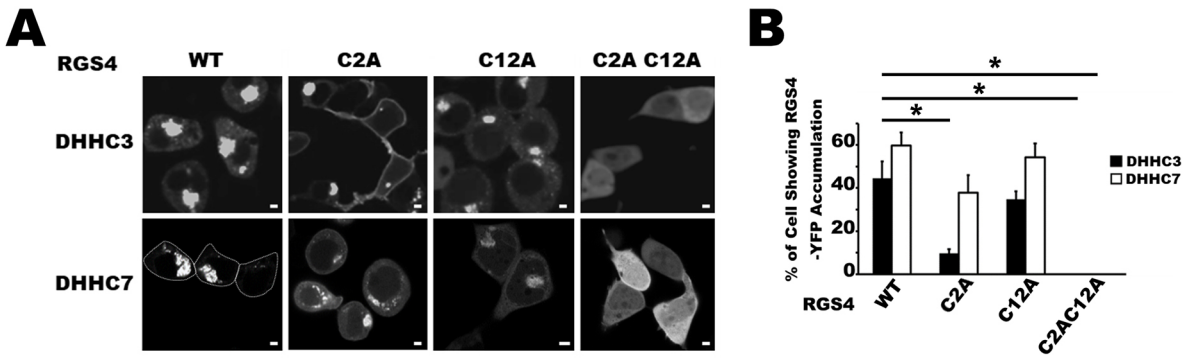

Fig. 3. The palmitoyl Co-A transferases DHHC3 and DHHC7 require N-terminal Cys2 and Cys12 residues in RGS4 to control its intracellular trafficking and substrate trapping. (A) Confocal microscopy pictures of wild-type RGS4–YFP (WT) and N-terminal cysteine mutants, C2A, C12A, C2AC12A co-expressed with DHHC3 or DHHC7, as indicated. Scale bars: 1 µm. The data are representative of at least three independent experiments carried out on separate days. (B) Histogram plot showing the mean±s.e.m. percentage of transfected cells where RGS4–YFP (or the indicated mutant) is directed to large intracellular membrane structures deep in the cytosol when co-expressed with DHHC3 or DHHC7. The data are representative of three independent experiments carried out on separate days (*n*=3). **P*<0.05 (two-way ANOVA and Tukey's post-hoc test).

Journal of Cell Science (2020) 133, jcs241034. doi:10.1242/jcs.241034

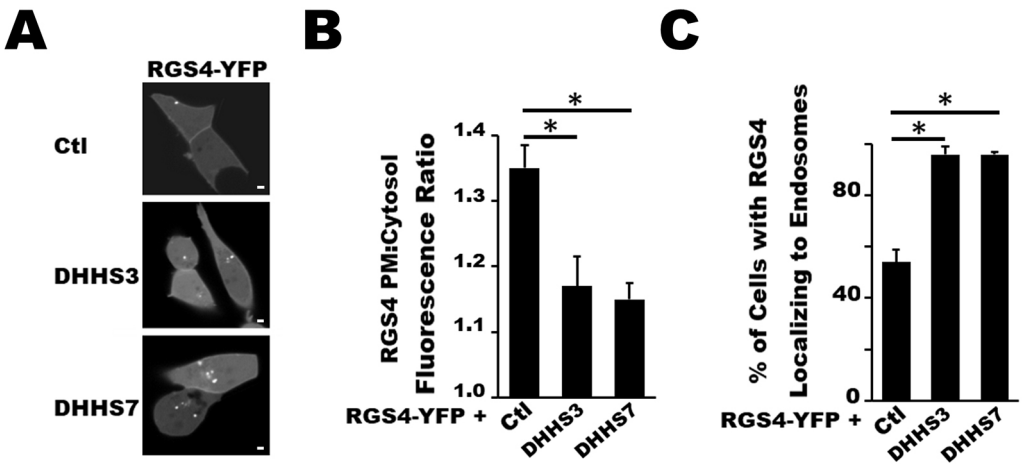

Fig. 4. The palmitoyl CoA-transferase activity of endogenous DHHC3 and DHHC7 control intracellular trafficking and distribution of RGS4. (A) Confocal microscopy showing cellular localization of RGS4–YFP with vector control or specific dominant-negative (DHHS) constructs for DHHC3 and DHHC7. Scale bars: 1 µm. (B) Histogram showing the mean±s.e.m. of plasma membrane to cytosol expression ratio for RGS4–YFP following co-expression with the indicated DHHC dominant-negative constructs as in A. (C) Histogram shows the mean±s.e.m. percentage of cells with RGS4–YFP localizing at endosomes following co-expression with the indicated DHHC dominant-negative constructs as in A and B. In all panels, the data are representative of three independent experiments carried out on separate days (*n*=3). **P*<0.05 (one-way ANOVA and Tukey's post-hoc test).

intracellular Gαi3 and increasing Bcl-2 phosphorylation, DHHS3 showed a much more potent effect than DHHS7 and empty vector (Fig. 6). This data highlights the extent to which the prevalence of RGS4 on TGN-38-positive endosomes affects P-Bcl-2 levels. Although both DHHS3 and DHHS7 roughly double the proportion of cells containing RGS4-labeled endosomes compared to control vector (Fig. 4C), the percentage of those RGS4-labeled endosomes colocalizing with TGN38 is higher for DHHS3 (58%) and control (64%) compared to DHHS7 (36%) (Fig. 5). These ratios would predict that P-Bcl-2 levels for the samples should be DHHS3 ≫DHHS7>vector control, precisely as is observed (Fig. 6). Notably, this effect was observed only for wild-type RGS4, but not for its catalytically dead control [RGS4(EN-AA)], which we have previously shown cannot inhibit Gαi activity (Bastin et al., 2015). Together, these data are consistent with the notion that DHHC3 inhibition increases the presence of RGS4 on the intracellular compartment, trapping RGS4 on TGN38-containing endosomes that also contain Gαi3, and that it is the TGN38-marked intracellular vesicle pool that is important for regulating Bcl-2 phosphorylation in our system.

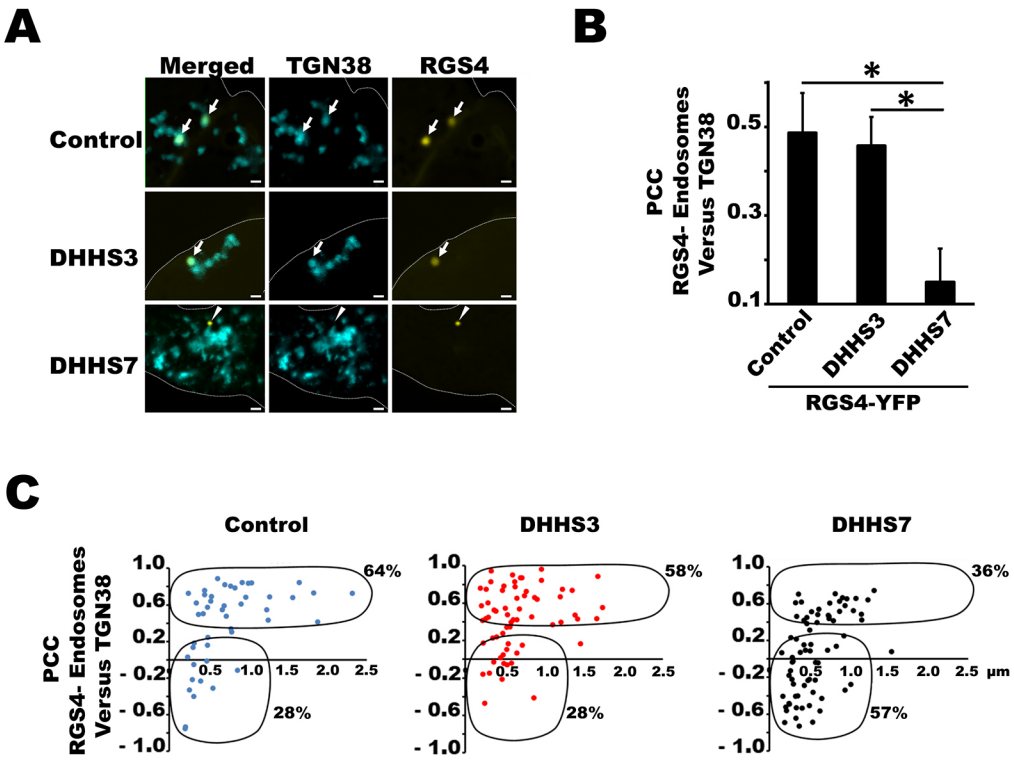

Fig. 5. The palmitoyl-CoA transferase activity of endogenous DHHC3 and DHHC7 direct RGS4 into discreet intracellular endosome pools. (A) Confocal microscopy showing cellular localization of RGS4–YFP following its co-expression with vector control or the indicated dominant-negative (DHHS) constructs for DHHC3 and DHHC7. Arrowheads and arrows indicate RGS4–YFP-containing endo-membranes which positively or negatively co-localize with TGN38-CFP, respectively. White dashed lines show the outline of the cells displayed. Scale bars: 1 µm. (B) Histogram shows the mean±s.e.m. of colocalization of RGS4 on endosomes with TGN38 as measured by determining the PCC, following co-expression with vector control or the indicated dominant-negative (DHHS) constructs for DHHC3 and DHHC7. (C) Scatter plots to relate the PCC value of endosomes positive for RGS4 and TGN38 to endosomal size (diameter). The data are representative of three independent experiments carried out on separate days (*n*=3). **P*<0.05 (one-way ANOVA and Tukey's post-hoc test).

Journal of Cell Science (2020) 133, jcs241034. doi:10.1242/jcs.241034

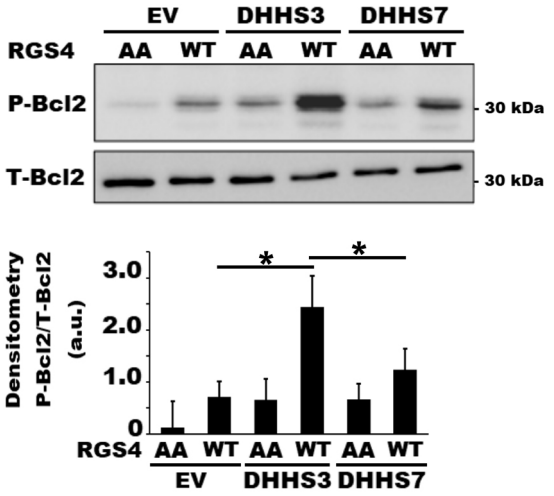

Fig. 6. Inhibition of endogenous DHHC3 and DHHC7 differentially regulates RGS4- and Gαi3-mediated effects on intracellular P-Bcl-2 levels. The ability of transfected wild-type RGS4 (WT) and its inactive mutant RSS4-ENAA (AA) to inhibit endogenous Gαi3-mediated regulation of P-Bcl-2 levels was examined following their co-expression with the indicated dominant-negative DHHC isoforms or empty vector (EV). The upper panel shows western blots for phospho (P)- and total (T)-Bcl-2, while the lower panel contain the mean±s.e.m. quantification of P-Bcl-2:T-Bcl-2 ratios as in the legend of Fig. 1. Data are representative of three independent experiments carried out on separate days (n=3). *P<0.05 (one-way ANOVA and Tukey's post-hoc test).

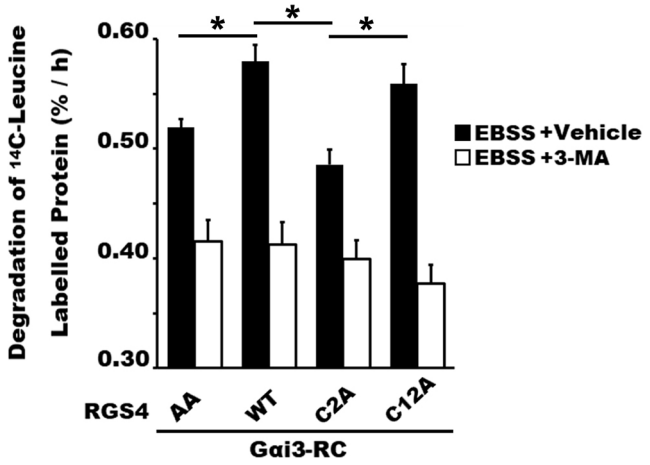

Fig. 7. RGS4 trafficking to TGN38-positive endosomes blocks Gαi3-RC-mediated inhibition of autophagic flux under nutrient-deprived conditions. Histogram shows the mean±s.e.m. of the degradation rate of [^{14}C]leucine-labeled long-lived proteins in cells transfected with Gαi3-RC and the indicated wild type (WT), inactive (AA), or N-terminal palmitoylation site mutants (C2A and C12A) of RGS4. The proportion of [^{14}C]leucine-labeled protein degraded by autophagy was indicated by the addition of 3-MA, an inhibitor of VPS34 and autophagy flux. The data are representative of at least three independent experiments carried out on separate days. *P<0.05 (two-way ANOVA and Tukey's post-hoc test).

Autophagy is regulated by Gαi3 and RGS4 from within discreet TGN38-marked compartments

As discussed above, Bcl-2 phosphorylation was previously shown to be an important step in the activation of autophagic signaling (Pattingre et al., 2009, 2005; Wei et al., 2008; He et al., 2012). Since RGS4 appears to regulate Bcl-2 phosphorylation on intracellular membranes, we asked whether our results might suggest that it has a role in the regulation of autophagic signaling via Gαi3. To test this possibility, we measured the degradation rate of long-lived proteins labeled with [^{14}C]leucine in our transfected cultures (Ogier-denis et al., 1996, 2000). As expected, nutrient starvation, a condition known to increase catabolism of long-lived proteins, significantly increased the rate of protein degradation compared to that seen in fed conditions (Fig. S7). Importantly, this phenotype was shown to be dependent on the activity of autophagy-initiating enzyme VPS34 (also known as PIK3C3), because its specific inhibitor, 3-MA, prevented these effects (Petiot et al., 2000) (Fig. S7). Transfection of RGS4 significantly increased the rate of long-lived protein degradation compared to the RGS-dead (RGS4-ENAA) construct, consistent with its ability to increase autophagic flux in those samples (Fig. 7). 3-MA eliminated the differences in flux between RGS4-ENAA and RGS4-WT in this assay (Fig. 7); these data support the idea that RGS4 activity regulates [^{14}C]leucine-labeled protein degradation mainly through the regulation of autophagy. Previously, we have also shown that RGS4-C2A does not colocalize with TGN38 on intracellular membranes, whereas RGS4-C12A specifically targeted TGN38-positive membrane pools (Bastin et al., 2012). Therefore, we used RGS4-C2A and RGS4-C12A as molecular tools to determine which pools of RGS4 could regulate Gαi3 inhibition and autophagic flux. Consistent with our data using DHHS proteins above, the RGS4 mutant that did not localize to TGN38-marked vesicle pools (RGS4-C2A) did not increase autophagic flux, whereas the RGS4 mutant that colocalized with TGN38 pools (RGS4-C12A) significantly increased autophagic activity (Fig. 7). Together, these data are consistent with the hypothesis that RGS proteins act to increase autophagic flux mediated by Gαi3 found on TGN38-positive endosomes.

Endogenous RGS4 enhances autophagy in adrenal glands

Finally, to test whether endogenous RGS4 could regulate autophagy in intact tissues *ex vivo*, we examined its effect(s) in adrenal glands from wild-type and RGS4-KO (LacZ-reporter) mice. LacZ staining confirmed very high expression levels of the *Rgs4* gene in the medulla of mouse adrenal glands (Fig. 8A). [^{14}C]leucine labeling studies revealed long-lived protein degradation rates were reduced in RGS4-KO compared to wild-type tissues exposed to nutrient starvation conditions, indicating markedly inhibited autophagy flux in the knockout tissues (Fig. 8B). Notably, treatment with the VPS34 inhibitor 3-MA abrogated the differences in long-lived protein degradation between RGS4-WT and -KO tissues, suggesting that RGS4 and Gαi3 are upstream of VPS34 in the autophagy signaling pathway.

DISCUSSION

Identification of a new Gαi3–JNK–Bcl-2 signaling axis in the control of cell stress signaling

Bcl-2 is widely known to act as an anti-apoptotic protein, while an increasing number of new roles have been identified for it in processes such as cell cycle progression, glucose and intracellular Ca^{2+} homeostasis and autophagy (Yamamoto et al., 1999; Bassik et al., 2004; Pattingre et al., 2005; Zinkel et al., 2006; He et al., 2012). Importantly, previous studies have revealed that Bcl-2 can be phosphorylated on serine and threonine residues within the non-structured loop between its BH3 and BH4 domains in response to various stress stimuli (Haldart et al., 1995; Yamamoto et al., 1999; Blagosklonny, 2001). While there remains some debate over whether such phosphorylation increases or decreases the anti-apoptotic potential of Bcl-2 (Haldart et al., 1995; Yamamoto et al.,

Journal of Cell Science (2020) 133, jcs241034. doi:10.1242/jcs.241034

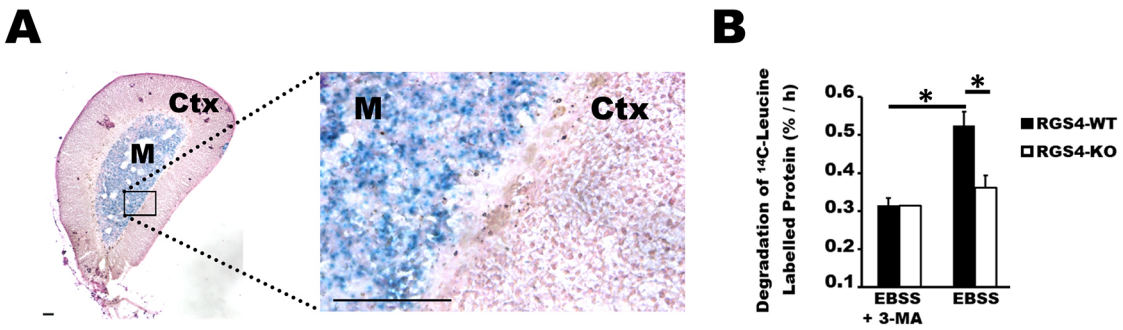

Fig. 8. Endogenous RGS4 expression promotes autophagy flux in adrenal glands. (A) Histochemical examination of RGS4 expression in adrenal glands of RGS4-KO/LacZ-reporter mouse on a C57Bl/6 background. Expression from the *Rgs4* gene is reported by nuclear-localized lacZ staining with nuclear Fast Red as a counterstain. 'M' and 'Ctx' denote adrenal gland medulla and cortex, respectively. The right panel shows a magnified region from the left panel. Scale bars: 0.5 mm. (B) Histogram showing the mean±s.e.m. of relative degradation rates of [^{14}C]leucine-labeled long-lived proteins in RGS4-WT and -KO adrenal glands exposed to nutrient-deprived conditions. The data are representative of three independent experiments run in duplicates and carried out on separate days (n=3). *P<0.05 (two-way ANOVA and Tukey's post-hoc test).

1999; Bassik et al., 2004; Deng et al., 2006; Chong et al., 2019), the majority of work suggests that phosphorylation of the Bcl-2 flexible loop domain is associated with its functional inactivation as both an anti-apoptotic and anti-autophagic protein in mammalian cells (Bassik et al., 2004; Wei et al., 2008; Blagosklonny, 2001; He et al., 2012).

In the case of autophagy regulation by Bcl-2, the serine/threonine stress kinase JNK has been shown to be critical for phosphorylation of its flexible loop domain following nutrient deprivation (Yamamoto et al., 1999; Wei et al., 2008). Bcl-2 phosphorylation promotes the release of Beclin-1 from Beclin-1–Bcl-2 heterodimeric complexes and allows Beclin-1 to associate with VPS34–Atg14 complexes to initiate autophagosome formation, a rate-limiting step in the autophagy pathway (Pattingre et al., 2005; Itakura et al., 2008; Zhong et al., 2009; Funderburk et al., 2010; Kang et al., 2011). Although Gαi3 and its regulators have been previously shown to regulate autophagic machinery in response to nutrient starvation (Ogier-denis et al., 1996, 2000; Pattingre et al., 2003; Garcia-marcos et al., 2011; Gohla et al., 2007), our data provides new mechanistic insight into this activity via their ability to control JNK activity and Bcl-2 phosphorylation from within specific intracellular membrane pools. It is reasonable to assume that similar regulatory effects might also modulate other stress signaling pathways such as ER stress (via IRE1α) (Cheng et al., 2014), organellar damage and toxin-induced reactive oxygen species (ROS) production, that have also been shown to stimulate autophagy via JNK activation (Bellot et al., 2013; Liu et al., 2015). Finally, although beyond the scope of this study, it will be of future interest to determine whether Gαi3 and RGS4 may similarly modulate the anti-apoptotic function of Bcl-2 via similar mechanisms. Indeed, the linkages between autophagy (a survival pathway) and apoptosis (a death pathway) remain an area of intense interest in cell biologic systems, and phosphorylated Bcl-2 may be one player at the interface between these two important cellular functions.

Gαi3 may integrate with JNK–Bcl-2 signaling at multiple control points

While we provide new evidence to support an intracellular Gαi3–JNK–Bcl-2 signaling pool as an integration point for intracellular stress signaling, it remains to be determined how Gαi3 can act as such a potent and specific regulator of intracellular JNK activity. One possibility is that Gαi/o proteins can inhibit specific adenylyl cyclase/cAMP pools and thus lower local PKA activity, which has been shown to activate JNK (Chen et al., 2007). The recent demonstration that Golgi-resident β1-adrenergic receptors in cardiac myocytes can activate localized cAMP-dependent hypertrophic signaling (Nash et al., 2019) highlights the need to study the role of Golgi-targeted Gαi3 (and other Gαs) as important mediators of intracellular signaling (Nash et al., 2019). Alternatively, a more generalized role for Gαi3 may relate to its involvement in Golgi membrane homeostasis and TGN-mediated secretion and membrane trafficking (Almeida et al., 1993; Aridor et al., 1993; Wilson et al., 1993; Kreft et al., 1999; Lo et al., 2015). Indeed, the Golgi-resident Gαi3 activator, GIV/Girdin, has been shown to regulate Arf1-mediated control of protein trafficking between the ER/ERGIC and Golgi, as well as to modulate Golgi stack organization and secretory capacity (Lo et al., 2015). Maintenance of constitutive Golgi secretion via Gαi3 activity could be expected to limit the levels of unfolded proteins, ER stress, and activation of stress-signaling kinases such as JNK. It is of interest that Gαi3, GIV/Girdin, RGS19, RGS4 and AGS3 have all been shown to localize to the Golgi and appear to play a role in membrane trafficking at the TGN or elsewhere (Almeida et al., 1993; Wylie et al., 1999; Sullivan et al., 2000; Lo et al., 2015; Bastin et al., 2012; Oner et al., 2013). The data herein suggest that the cycling of Gαi3 from GTP- to GDP-bound states could be a major determinant of the regulation of Bcl-2 phosphorylation status mediated by RGS4. These data would therefore suggest that regulation of Bcl-2 requires a transient interaction with Gαi3 partner(s) and effector(s) similar to that normally used by other small GTPases, such as Arf1, to mediate membrane trafficking events. It will, therefore, be of interest to determine whether Gαi3 and Arf1 show overlapping functions as regulators of autophagy.

The importance of targeting RGS4 and other Gαi3 regulators to TGN-marked membranes

We have previously shown that proper palmitoylation of RGS4 on Cys2 and Cys12 is critical for its normal trafficking and localization to both the plasma membrane and intracellular membrane pools, especially those marked by the trans-Golgi protein TGN38 (Bastin et al., 2012). Moreover, we demonstrated that RGS4 localization to TGN38-containing pools profoundly promoted intracellular JNK activation in nutrient-starved conditions (Bastin et al., 2015), a phenotype that we herein link to increased Bcl-2 phosphorylation and autophagic signaling. The differential regulation of JNK and Bcl-2 by RGS4 and Gαi3 between these different intracellular compartments suggests that different effectors are involved. On the

other hand, while the primary focus of this work was to study the role of RGS4 as a Gαi3 regulator, we do not exclude the possibility that other RGS proteins with highly similar (such as RGS5 and RGS16) or different (RGS19) palmitoylation footprints might be able to regulate P-Bcl-2 levels in a similar manner. The other interesting aspect of this study was the possible role that Golgi-resident DHHCs and other palmitoylating enzymes may play on the regulation of Gαi3–JNK–Bcl-2 signaling under normal and pathogenic conditions. It seems likely that alterations in levels of palmitoyl-CoA substrate, such as might be seen in high-fat feeding conditions, could have important effects on the localization and function of important mediators of metabolic function. Dysregulation of these pathways could lead to reduced clearance of lipids and other waste products through lipophagic and autophagic mechanisms, resulting in a cell-toxic build-up of these materials.

Gαi3 may connect Golgi- and plasma membrane-dependent growth factor signaling

It may not be a coincidence that growth factor receptor signaling activates Gαi3 at the plasma membrane (PM) and can also act as a potent inhibitor of both autophagic and apoptotic signaling. Indeed, both GIV/Girdin and Gαi3 were shown to be required for insulin–insulin receptor signaling-mediated inhibition of autophagy in cell (Garcia-marcos et al., 2011) and intact animal (Gohla et al., 2007) models. Moreover, growth factor (insulin or EGFR) activation was shown to direct Gαi3 toward intracellular pools of GIV/Girdin, whereas starvation conditions directed it toward AGS3- and LC3-containing membranes (Garcia-marcos et al., 2011). It is tempting to speculate that such growth factor signaling at the cell surface may also be linked to the intracellular Gαi3–JNK–Bcl-2 signaling complexes we show can be localized on TGN38-marked membranes. Indeed, crosstalk signaling between growth factor receptors and Golgi function have been previously reported by a number of other groups (Blagoveshchenskaya et al., 2008; Weller et al., 2010). Aside from the ability of Gαi3 (and its regulators) to traffic between PM and Golgi domains, one molecule in particular, AKT (protein kinase B) has been shown to link growth factor stimuli to intracellular signaling domains. AKT can be activated at the plasma membrane by growth factor receptor signaling pathways that require Gαi3 and GIV-dependent mechanisms (Ghosh et al., 2008; Garcia-marcos et al., 2011, 2010). Notably, activated AKT can directly phosphorylate intracellular Beclin-1 to direct it away from (VPS34/Atg14) autophagy-activating pathways and redirect it toward 14-3-3–vimentin complexes during tumorigenesis (Wang et al., 2012). The extent to which AKT might also modulate other intracellular proteins that control Golgi secretion, homeostasis, or JNK or Bcl-2 activity at or near the ER–Golgi interface remains to be determined. It is of interest that AKT has been shown to directly phosphorylate Sec24, an essential coat protein II (COPII) component involved in ER-to-Golgi trafficking (Sharpe et al., 2011), and that COPII-marked vesicles have been recently implicated in the expansion of the autophagic phagophore (Davis et al., 2016; Rabouille, 2019).

MATERIALS AND METHODS

Materials

HEK293 cells (tsA-201 derivative) were a kind gift from Zhong-Ping Feng (University of Toronto, Canada). All tissue culture media and transfection reagents were purchased from Invitrogen (Thermo Fisher Scientific) and Roche Scientific, respectively. Human Gαi3 gene guide RNA constructs for CRISPR deletion studies were a kind gift from Asuka Inoue, Tokohu University, Sendai, Miyagi, Japan. The Gαi3–CFP construct was a kind gift from Catherine Berlot (Weis Center for Research, Geisinger Clinic, Danville, PA). AGS3-GFP was generously provided by Stephen Lanier (University of South Carolina, SC). TGN38-cerulean were from Jennifer Lippincott Schwartz (National Institutes of Health, Bethesda, MD). Bcl-2 construct was kindly provided by David Andrews (University of Toronto, Canada). HA-tagged DHHC3, DHHC5, DHHC7 and DHHC21 were generously provided by Masaki Fukata (National Institute for Physiological Sciences, Okazaki, Japan). Antibodies against T-Bcl-2 and P-Bcl-2 were purchased from Cell Signaling with the respective catalog numbers: # 2870P and # 2827L. Antibodies against HA-tag were purchased from Roche (Cat. # 11666606001). Horseradish peroxidase-coupled anti-rabbit-IgG secondary antibodies were from Cell Signaling (Cat. # 70745). Alexa Fluor 405 cross adsorbed to secondary goat anti-mouse IgG antibodies were from Thermo Fisher Scientific (Cat. # A-31553). Unless otherwise stated all other reagents and chemicals were from Sigma-Aldrich.

Cell culture

HEK293 cells were grown in complete medium: Dulbecco's modified Eagle's medium (DMEM; Gibco, Cat. # 11995-065), supplemented with 10% (v/v) heat-inactivated fetal bovine serum (Gibco, Cat. # 12483020), 2 mM glutamine, (Thermo Fisher Scientific, Cat. # 25030081) with 10 µg/ml streptomycin, and 100 units/ml penicillin (Thermo Fisher Scientific, Cat. # 15140122) at 37°C in a humidified atmosphere with 5% CO_2. HEK293 cells (tsA-201 derivative) stably expressing an EYFP-tagged RGS4 were grown in complete medium supplemented with 0.5 mg/ml active G-418 (Geneticin, Sigma Aldrich). EBSS was used as a starvation medium (Thermo Fisher Scientific, Cat. # 14155-063), 200 mg/l of both $CaCl_2$ and $MgCl_2$ were added to the solution as well as 0.1% BSA and 0.2% FBS.

siRNA

Transient transfection of siRNA using Lipofectamine RNAiMAX (Invitrogen, Cat. # 13778-075) was performed according to manufacturer's protocols. All siRNAs were purchased from Dharmacon RNAi Technologies (part of Thermo Fisher Scientific). For human DHHC3 and DHHC7 knockdown, the following target sequences were used: DHHC3, 5′-CAUCGCGAGAGUUUACAGUUG-3′, DHHC7, 5′-GCCC-GUGGGUGAACAAUUG-3′. The negative control siRNA used was siGENOME Non-Targeting siRNA #2 (Cat. # D001210-02-05).

Molecular biology

For subcellular localization studies, RGS4–YFP, and RGS domain and cysteine point mutations expression plasmids were generated in the pEYFP-C1 as described previously (Bastin et al., 2012). Gαi3-G184S-CFP, Gαi3-R178C-CFP and Gαi3-Q204L-CFP were created by site-directed mutagenesis methods using the forward strand primers 5′-AGAGTGAAG-ACCACATCGATAGTAGAAACACAT-3′, 5′-CCAACTCAGCCAGATG-TTCTTCGGACATGT-3′ and 5′-AGATGTTTGATGTAGGAGGCC-TAAGATCAGAACGAAAAA-3′, respectively, together with their reverse complements. The Gq/11-selective RGS4 mutant [RGS2 'triple (3x)'] mutant was created using primers: K170E, 5′-TACCGCCGCTTCCTCGAGTCTC-GATTCTAT-3′, D163N, 5′-AACCTGATGGAGAAGAATTCCTACCGC-CGCT-3′, S85C, 5′-TTTCTTGAAGTCTGATGAGTACTGTGGAGGAG-AATATTG-3′. Point mutations to convert DHHCs into dominant-negative DHHS 3, 5, 7 and 21 were generated by site-directed mutagenesis methods using the respective forward strand primers 5′-AGATGGATCACCACTCT-CCATGGGTCAACAACTGT-3′, 5′-AATTTGACCATCACTCCCCATGG-GTAAACAACTGT- 3′, 5′-AGATGGACCATCACTCCCCATGGGTGAA-CAACTGC-3′, 5′-GGATGGACCATCACTCTCCATGGATAAACAATT-GT-3′ together with their reverse complements. All plasmid constructs were purified using the Endofree Maxi kit (Qiagen, Cat. # 12362) and verified by sequencing of the complete protein-coding region.

SDS-PAGE and western blotting

HEK293 cells were plated at 50% confluence in tissue culture-treated dishes and transfected overnight with 1 µg of indicated cDNA constructs or 0.5 µg for Bcl-2 (the amount of Bcl-2 was carefully titrated to allow its detection while avoiding any deleterious effects on cell growth and viability) and

2.5 µl of X-tremegene HP transfection reagent according to the manufacturer's instructions (Merck, Cat. # 6366546001). After 24 h, the samples were collected using two-times concentrated Laemmli buffer, and the samples were then sonicated on ice. Protein samples were then separated by running 12% PAGE gels in denaturing conditions (SDS and DTT). Then, the proteins were transferred to nitrocellulose membrane (Trans-Blot, BioRad). Membranes were blocked for 1 h with Tris-buffered saline with 0.1% Tween-20 (TBST) and 5% bovine serum albumin (BSA). Primary antibodies were diluted at 1:1000 in TBST containing 5% BSA and incubated with membranes overnight at 4°C before removing by washing. Horseradish peroxidase linked-secondary antibodies were diluted (1:2000) in TBST with 5% BSA was added for 2 h, before washing and signal detection using Super Signal West Pico Chemiluminescent Substrate (Thermo Fisher Scientific). Western blots were analyzed by densitometry using Image J (Fiji) software analysis.

Generation of HEK Gαi3-KO HEK cells

Cas9-mediated knockout of $G\alpha_{i3}$ in HEK293T cells was performed as previously described (Ran et al., 2013). Briefly, HEK293T cells were transfected with plasmid pSpCas9(BB)-2A-GFP containing a single-guide RNA 5′-AGCTTGCTTCAGCAGATCCAGGG-3′ targeted to exon 4 of Gαi3-encoding gene. At 24 h post-transfection, positively transfected cells were selected by flow-assisted cell sorting and seeded with a singular cell being placed in each well of a 96-well plate to facilitate expansion of each clone. Effective knockout of $G\alpha_{i3}$ by indel mutations in each clone was confirmed by restriction digest of genomic DNA, western blot analysis of whole-cell lysates and by Sanger sequencing of clone mRNA. Once the cells were generated, they were checked for mycoplasma contamination.

Quantitative real-time PCR and analysis

Total RNA was extracted from HEK201 cells using TRIzol reagent (Invitrogen Life Technologies). All quantitative RT-PCR was performed using an ABI Prism 7900 HT (Applied Biosystems) using the Sybr Green detection system. First, 2 µg of total RNA was reverse-transcribed with random hexamer primers using the Superscript III kit (Invitrogen Life Technologies) following the manufacturer's protocols. cDNA was diluted to a final concentration of 1 ng/µl. Then, 2 µl of this mixture was used as template for real-time PCR quantification. DHHC expression was evaluated in each cDNA sample as indicated. Primers were validated using primer validation curves (User Bulletin No. 2, Perkin Elmer Life Sciences). 5′ PCR primers for housekeeping genes GAPDH and 18S were used as normalizing controls. Refer to Table S1 for list of all 5′ PCR primers used. A no-RT and no template control sample were included for each primer set. Data were analyzed using the comparative CT method (User Bulletin No. 2, Perkin Elmer Life Sciences). The CT for each sample was manipulated first to determine the ΔCT [(average CT of sample triplicates for the gene of interest) – (average CT of sample triplicates for the normalizing gene)] and second to determine the ΔΔCT [(ΔCT sample)-(ΔCT for the calibrator sample)]. Values are expressed in log scale and the relative mRNA levels are presented by conversion to a linear value using $2-\Delta\Delta CT$.

Confocal microscopy

HEK293 cells were plated at 50% confluence in tissue culture-treated microscopy dishes (Ibidi, Cat. # 81156) and transfected overnight with 1 µg of indicated cDNA constructs to be tested using 2.5 µl of Xtremegene HP transfection reagent according to the manufacturer's instructions (Merck, Cat. # 6366546001). After 24 h, dishes were examined by confocal microscopy, which was performed on 70–90% confluence live cells at 37°C using an Olympus FluoView 1000 laser-scanning confocal microscope in a 5% CO_2 atmosphere. Images represent a single equatorial plane on the basal side of the cell obtained with a 60× oil objective, 1.4 numerical aperture. For where it applies, a 405 nm diode lazer was used to excite CFP and 515 nm Multiline Argon Laser was used to excite YFP. Emission wavelength parameters of each were matched to the appropriate bandpass emission filters, and where more than one fluorescent channel was examined in a single cell, the possibility of bleed through fluorescence was excluded prior to evaluation. Confocal images were processed with Fluoview A-1000 software and Microsoft Office 2013. Quantification of plasma and endo-membrane RGS4 localization was performed by a researcher who was blind to the identity of sample (for capture of data and during data analysis), with membrane:cytosol ratios measured using the Image J software package and the Pearson correlation coefficient (PCC) for each endosome was calculated by the Fluo-View software; regions of interest containing RGS4–YFP endosomes were manually selected to quantify the PCC between each RGS4 and TGN38 endosomes (not as whole cell/field).

Immunofluorescence

A 40 µl volume of HEK 293 cells were plated in each well of BD-Falcon #354108. Transfection using Fugene (Roche #11 988 387 001) was performed simultaneously following manufacturer's instructions. The next day, the cells were rinsed once using 1 M PBS (containing Mg^{2+} and Ca^{2+} for this whole protocol) (Sigma #D8662). Then they were fixed using 4% paraformaldehyde for 15 min at room temperature. Two rinsings were applied using PBS. Membranes were permeabilized using 0.2% Triton X-100 diluted in PBS, for 10 min at room temperature. 5% BSA and 0.1% Triton X-100 were used for overnight blocking at 4°C. Then one rinsing was applied using pre-chilled PBS. Primary antibody was a mouse anti-HA antibody (Roche # 11 666 606 101), dilution 1:1000 was applied overnight at 4°C. Six rinsings were applied using pre-chilled PBS. Then a goat anti mouse secondary antibody (Invitrogen #A21049) was used at a dilution 1:500 at room temperature for 30 min. Prolong gold antifade reagent was applied to the slide prior to microscopy (Invitrogen #P36930).

Animals

All experiments conformed to the Guide for the Care and Use of Laboratory Animals published by the US National Institutes of Health (NIH Publication No. 85-23, revised 1996), Institutional Guidelines and the Canadian Council on Animal Care. The RGS4 knockout/LacZ-reporter mouse was reported previously (Cifelli et al., 2008). Briefly, an *Rgs4*-null locus was created with an IRES LacZ-Neo cassette inserted to delete 58 bp of coding sequence and the entire first intron. Both female and male mice were used and were of 10–16 weeks of age.

LacZ staining

Adrenal glands were isolated rapidly from euthanized animals and washed in pre-chilled PBS. Samples were equilibrated by 30% (w/v) sucrose and immersed in OCT compound before freezing in liquid nitrogen. Cryosections (15–20 µm) were mounted on surface-treated glass slides, post-fixed briefly, stained with nuclear fast red and photographed on a Nikon Eclipse E-600 dissecting microscope and a Hamamatsu Digital Camera C4742-95 and Simple PCI Version 5.3.0.1102 (Compix, Inc Imaging Systems). In adrenal gland preparation samples, slices were fixed in 10% formalin post cryosectioning for 15 min on ice. Development of the LacZ stain was achieved with appropriate incubation time at 37°C with X-gal solution [0.2% X-gal (4-chloro-5-bromo-3-indolyl-β-galactopyranoside), 2 mM $MgCl_2$, 0.02% Nonidet P-40, 0.01% SDS, 5 mM $K_3Fe(CN)6$ and 5 mM $K_4Fe(CN)_6$]. Slices were placed in a humidified chamber at 37°C until desired color development, washed in PBS and counterstained with Nuclear fast Red. Prior to mounting, samples were then washed three times repeatedly in PBS, and dehydrated with an ethanol series followed by three successive treatments with Xylene.

Long-lived protein assay

HEK293 cells were transiently transfected with the indicated clones. Intact adrenal glands (two per genotype per experiment) were extracted as described above and treated similarly to HEK293 cells as follows. Cells or tissues were labeled overnight with 0.2 µCi/ml of [^{14}C]leucine (Perkin Elmer Cat. # NEC291EU050UC) in DMEM-F12-10% FBS medium. Following four PBS washes to eliminate the excess of label, cells or tissues were incubated for 1 h at 37°C with EBSS containing 0.1% BSA, 0.1% FBS and 10 mM cold valine (chase medium) to allow for degradation of short-lived proteins. Next, the chase medium was added again with and without 10 mM 3-MA for an additional 24 h for HEK293 cells and 6 h for adrenal glands to allow for degradation of long-lived proteins. Medium and cell

fractions were collected separately. Cells or tissues were washed once on ice with PBS to remove most traces of medium containing radioactivity remaining. Then both medium and cells or tissues were treated with ice-cold trichloroacetic acid (TCA; 10%) and tungstenic acid (1%) were added to both medium and cell fractions. The TCA-soluble fraction was collected as the long-lived protein degraded fraction, whereas the insoluble material was collected as the non-degraded fraction. Liquid scintillation counting was performed using EcoscintA Cat. # LS-273 from National Diagnostics. The ratio of the soluble:insoluble ^{14}C counts was used as an indicator of the rate of long-lived protein degradation.

Data collection, management and statistical analysis

At the outset of each series of microscopy experiments, the experimenter was blind to the identity of the transfectants until data collection and analysis were completed. Where indicated, Student's *t*-test analysis, or one-way and two-way ANOVA with Tukey's post-hoc analysis were used to analyze the experimental results. $*P<0.05$ was considered significant. Error bars depict standard errors of the mean (s.e.m.) for all graphs.

Acknowledgements

We are grateful to Hangjun Zhang In the Ted Rogers Centre for Heart Research, Translational Biology and Engineering Program at the University of Toronto for mouse breeding and genotyping assistance, and Edouard Al-Chami (Clinton Robbins laboratory at the Toronto General Hospital Research Institute, Peter Munk Cardiac Centre, Toronto, ON) for assistance with fluorescence activated cell sorting of CRISPR-GFP cells. Guillaume Bastin was funded by a Postdoctoral Research Fellowship from the Heart and Stroke/Richard Lewar Centre of Excellence in Cardiovascular Research.

Competing interests

The authors declare no competing or financial interests.

Author contributions

Conceptualization: G.B., K.D., S.P.H.; Methodology: G.B., K.D., D.L., A.L.C.T., K.L., S.P.H.; Validation: G.B., K.D., D.L.; Formal analysis: G.B., K.D., D.L., S.-H.L.; Resources: S.P.H.; Writing - original draft: G.B.; Writing - review & editing: G.B., S.P.H.; Supervision: S.P.H.; Funding acquisition: S.P.H.

Funding

Project support for this work came from Operating Grants from the Canadian Institutes of Health Research (MOP-106670), Grants-in-Aid Program of the Heart and Stroke Foundation of Canada (T6799) and seed funding from the Ted Rogers Centre for Heart Research, Translational Biology and Engineering Program.

Supplementary information

Supplementary information available online at
http://jcs.biologists.org/lookup/doi/10.1242/jcs.241034.supplemental

Peer review history

The peer review history is available online at
https://jcs.biologists.org/lookup/doi/10.1242/jcs.241034.reviewer-comments.pdf

References

Almeida, J. B. De, Doherty, J., Ausiello, D. A. and Stow, J. L. (1993). Binding of the cytosolic p200 protein to Golgi membranes is regulated by heterotrimeric G proteins. *J. Cell Sci.* **106**, 1239-1248.

Aridor, M., Rajmilevich, G., Beaven, M. A. and Sagi-Eisenberg, R. (1993). Activation of exocytosis by the heterotrimeric G protein Gi3. *Science* **262**, 1569-1572. doi:10.1126/science.7504324

Bassik, M. C., Scorrano, L., Oakes, S. A., Pozzan, T. and Korsmeyer, S. J. (2004). Phosphorylation of BCL-2 regulates ER $Ca2^+$ homeostasis and apoptosis. *EMBO J.* **23**, 1207-1216. doi:10.1038/sj.emboj.7600104

Bastin, G., Singh, K., Dissanayake, K., Mighiu, A. S., Nurmohamed, A. and Heximer, S. P. (2012). Amino-terminal cysteine residues differentially influence RGS4 protein plasma membrane targeting, intracellular trafficking, and function. *J. Biol. Chem.* **287**, 28966-28974. doi:10.1074/jbc.M112.345629

Bastin, G., Yang, J. Y. and Heximer, S. P. (2015). Gαi3-dependent inhibition of JNK activity on intracellular membranes. *Front. Bioeng. Biotechnol.* **3**, 1-9. doi:0.3389/fbioe.2015.00128

Bellot, G. L., Liu, D. and Pervaiz, S. (2013). ROS, autophagy, mitochondria and cancer: Ras, the hidden master? *Mitochondrion* **13**, 155-162. doi:10.1016/j.mito.2012.06.007

Berman, D. M., Kozasa, T. and Gilman, A. G. (1996a). The GTPase-activating protein RGS4 stabilizes the transition state for nucleotide hydrolysis. *J. Biol. Chem.* **271**, 24-26. doi:10.1074/jbc.271.44.27209

Berman, D. M., Wilkie, T. M. and Gilman, A. G. (1996b). GAIP and RGS4 are GTPase-activating proteins for the Gi subfamily of G protein α subunits. *Cell* **86**, 445-452. doi:10.1016/S0092-8674(00)80117-8

Blagosklonny, M. V. (2001). Unwinding the loop of Bcl-2 phosphorylation. *Leukemia* **15**, 869-874. doi:10.1038/sj.leu.2402134

Blagoveshchenskaya, A., Cheong, F. Y., Rohde, H. M., Glover, G., Knödler, A., Nicolson, T., Boehmelt, G. and Mayinger, P. (2008). Integration of Golgi trafficking and growth factor signaling by the lipid phosphatase SAC1. *J. Cell Biol.* **180**, 803-812. doi:10.1083/jcb.200708109

Chen, D., Reierstad, S., Lin, Z., Lu, M., Brooks, C., Li, N., Innes, J. and Bulun, S. E. (2007). Prostaglandin E2 induces breast cancer related aromatase promoters via activation of p38 and c-Jun NH2 -terminal kinase in adipose fibroblasts. *Cancer Res.* **67**, 8914-8923. doi:10.1158/0008-5472.CAN-06-4751

Cheng, X., Liu, H., Jiang, C., Fang, L., Chen, C., Zhang, X.-D. and Jiang, Z.-W. (2014). Connecting endoplasmic reticulum stress to autophagy through IRE1/JNK/beclin-1 in breast cancer cells. *Int. J. Mol. Med.* **34**, 772-781. doi:10.3892/ijmm.2014.1822

Chong, S. J. F., Lai, J. X. J. H., Qu, J., Hirpara, J., Kang, J., Swaminathan, K., Loh, T., Kumar, A., Vali, S., Abbasi, T. et al. (2019). A feedforward relationship between active Rac1 and phosphorylated Bcl-2 is critical for sustaining Bcl-2 phosphorylation and promoting cancer progression. *Cancer Lett.* **457**, 151-167. doi:10.1016/j.canlet.2019.05.009

Cifelli, C., Rose, R. A., Zhang, H., Voigtlaender-Bolz, J., Bolz, S.-S., Backx, P. H. and Heximer, S. P. (2008). RGS4 regulates parasympathetic signaling and heart rate control in the sinoatrial node. *Circ. Res.* **103**, 527-535. doi:10.1161/CIRCRESAHA.108.180984

Coleman, D., Berghuis, A., Lee, E., ME, L., Gilman, A. and Sprang, S. (1994). Structures of active conformations of Gi alpha 1 and the mechanism of GTP hydrolysis. *Science* **265**, 1405-1412. doi:10.1126/science.8073283

Davis, S., Wang, J., Zhu, M., Stahmer, K., Lakshminarayan, R., Ghassemian, M., Jiang, Y., Miller, E. A. and Ferro-Novickl, S. (2016). Sec24 phosphorylation regulates autophagosome abundance during nutrient deprivation. *Elife* **5**, e21167. doi:10.7554/eLife.21167

Deng, X., Gao, F., Flagg, T., Anderson, J. and May, S. W. (2006). Bcl2's flexible loop domain regulates p53 binding and survival. *Mol. Cell. Biol.* **26**, 4421-4434. doi:10.1128/MCB.01647-05

Fukata, M., Fukata, Y., Adesnik, H., Nicoll, R. A. and Bredt, D. S. (2004). Identification of PSD-95 palmitoylating enzymes. *Neuron* **44**, 987-996. doi:10.1016/j.neuron.2004.12.005

Fukata, Y., Iwanaga, T. and Fukata, M. (2006). Systematic screening for palmitoyl transferase activity of the DHHC protein family in mammalian cells. *Methods* **40**, 177-182. doi:10.1016/j.ymeth.2006.05.015

Funderburk, S. F., Wang, Q. J. and Yue, Z. (2010). The Beclin 1 – VPS34 complex – at the crossroads of autophagy and beyond. *Trends Cell Biol.* **20**, 355-362. doi:10.1016/j.tcb.2010.03.002

Garcia-marcos, M., Ghosh, P., Ear, J. and Farquhar, M. G. (2010). A structural determinant that renders Gαi sensitive to activation by GIV/Girdin is required to promote cell migration. *J. Biol. Chem.* **285**, 12765-12777. doi:10.1074/jbc.M109.045161

Garcia-marcos, M., Ear, J., Farquhar, M. G. and Ghosh, P. (2011). A GDI (AGS3) and a GEF (GIV) regulate autophagy by balancing G protein activity and growth factor signals. *Mol. Biol. Cell* **22**, 673-686. doi:10.1091/mbc.e10-08-0738

Ghosh, P., Garcia-Marcos, M., Bornheimer, S. J. and Farquhar, M. G. (2008). Activation of Gi3 triggers cell migration via regulation of GIV. *J. Cell Biol.* **182**, 381-393. doi:10.1083/jcb.200712066

Gohla, A., Klement, K., Piekorz, R. P., Pexa, K., Vom Dahl, S., Spicher, K., Dreval, V., Haussinger, D., Birnbaumer, L. and Nurnberg, B. (2007). An obligatory requirement for the heterotrimeric G protein Gi3 in the antiautophagic action of insulin in the liver. *Proc. Natl. Acad. Sci. USA* **104**, 3003-3008. doi:10.1073/pnas.0611434104

Haldart, S., Jena, N. and Croce, C. M. (1995). Inactivation of Bcl-2 by phosphorylation. *Proc. Natl. Acad. Sci. USA* **92**, 4507-4511. doi:10.1073/pnas.92.10.4507

He, C., Bassik, M. C., Moresi, V., Sun, K., Wei, Y., Zou, Z., An, Z., Loh, J., Fisher, J., Sun, Q. et al. (2012). Exercise-induced Bcl2-regulated autophagy is required for muscle glucose homeostasis. *Nature* **481**, 511-515. doi:10.1038/nature10758

Hepler, J. R. and Gilman, A. G. (1992). G proteins. *Trends Biochem. Sci.* **17**, 383-387. doi:10.1016/0968-0004(92)90005-T

Hewavitharana, T. and Wedegaertner, P. B. (2012). Non-canonical signaling and localizations of heterotrimeric G proteins. *Cell. Signal.* **24**, 25-34. doi:10.1016/j.cellsig.2011.08.014

Huang, K., Yanai, A., Kang, R., Arstikaitis, P., Singaraja, R. R., Metzler, M., Mullard, A., Haigh, B., Gauthier-Campbell, C., Gutekunst, C.-A. et al. (2004). Huntingtin-interacting protein HIP14 is a palmitoyl transferase involved in palmitoylation and trafficking of multiple neuronal proteins. *Neuron* **44**, 977-986. doi:10.1016/j.neuron.2004.11.027

Itakura, E., Kishi, C., Inoue, K. and Mizushima, N. (2008). Beclin 1 forms two distinct phosphatidylinositol 3-kinase complexes with mammalian Atg14 and UVRAG. *Mol. Biol. Cell.* **19**, 5360-5372. doi:10.1091/mbc.e08-01-0080

Kang, R., Zeh, H. J., Lotze, M. T. and Tang, D. (2011). The Beclin 1 network regulates autophagy and apoptosis. *Cell Death Differ.* **18**, 571-580. doi:10.1038/cdd.2010.191

Kreft, M., Gasman, S., Chasserot-golaz, S., Kuster, V., Rupnik, M., Sikdar, S. K., Bader, M. and Zorec, R. (1999). The heterotrimeric Gi3 protein acts in slow but not in fast exocytosis of rat melanotrophs. *J. Cell Sci.* **112**, 4143-4150.

Le-niculescu, H., Niesman, I., Fischer, T., DeVries, L. and Farquhar, M. G. (2005). Identification and characterization of GIV, a novel Gαi/s -interacting protein found on COPI, endoplasmic reticulum-golgi transport vesicles. *J. Biol. Chem.* **280**, 22012-22020. doi:10.1074/jbc.M501833200

Li, X., Wang, D., Chen, Z., Lu, E., Wang, Z., Li, X., Wang, D., Chen, Z., Lu, E., Wang, Z. et al. (2015). Gαi1 and Gαi3 regulate macrophage polarization by forming a complex containing CD14 and Gab1. *Proc. Natl. Acad. Sci. USA* **115**, 4731-4736. doi:10.1073/pnas.1503779112

Liu, J., Chang, F., Li, F., Fu, H., Wang, J., Zhang, S., Zhao, J. and Yin, D. (2015). Palmitate promotes autophagy and apoptosis through ROS-dependent JNK and p38 MAPK. *Biochem. Biophys. Res. Commun.* **463**, 262-267. doi:10.1016/j.bbrc.2015.05.042

Lo, I.-C., Gupta, V., Midde, K. K., Taupin, V., Lopez-Sanchez, I., Kufareva, I., Abagyan, R., Randazzo, P. A., Farquhar, M. G. and Ghosh, P. (2015). Activation of Gαi at the golgi by GIV/Girdin imposes finiteness in Arf1 signaling. *Dev. Cell* **33**, 189-203. doi:10.1016/j.devcel.2015.02.009

Michaelson, D., Ahearn, I., Bergo, M., Young, S. and Philips, M. (2002). Membrane trafficking of heterotrimeric G proteins via the endoplasmic reticulum and golgi. *Mol. Biol. Cell* **13**, 3294-3302. doi:10.1091/mbc.e02-02-0095

Nash, C. A., Wei, W., Irannejad, R. and Smrcka, A. V. (2019). Golgi localized β1-adrenergic receptors stimulate Golgi PI4P hydrolysis by PLCε to regulate cardiac hypertrophy. *eLife* **8**, e48167. doi:10.7554/eLife.48167

Ogier-denis, E., Houri, J., Bauvy, C. and Codogno, P. (1996). Guanine nucleotide exchange on heterotrimeric Gi3 protein controls autophagic sequestration in HT-29 cells. *J. Biol. Chem.* **271**, 28593-28600. doi:10.1074/jbc.271.45.28593

Ogier-denis, E., Pattingre, S., El Benna, J. and Codogno, P. (2000). Erk1/2-dependent phosphorylation of gα-interacting protein stimulates its GTPase accelerating activity and autophagy in human colon cancer cells. *J. Biol. Chem.* **275**, 39090-39095. doi:10.1074/jbc.M006198200

Ohno, Y., Kihara, A., Sano, T. and Igarashi, Y. (2006). Intracellular localization and tissue-specific distribution of human and yeast DHHC cysteine-rich domain-containing proteins. *Biochim. Biophys. Acta* **1761**, 474-483. doi:10.1016/j.bbalip.2006.03.010

Oner, S. S., Vural, A. and Lanier, S. M. (2013). Translocation of activator of G-protein signaling 3 to the golgi apparatus in response to receptor activation and its effect on the trans-golgi network. *J. Biol. Chem.* **288**, 24091-24103. doi:10.1074/jbc.M112.444505

Pattingre, S., De Vries, L., Bauvy, C., Chantret, I., Cluzeaud, F., Ogier-denis, E., Vandewalle, A. and Codogno, P. (2003). The G-protein regulator AGS3 controls an early event during macroautophagy in human intestinal HT-29 Cells. *J. Biol. Chem.* **278**, 20995-21002. doi:10.1074/jbc.M300917200

Pattingre, S., Tassa, A., Qu, X., Garuti, R., Liang, X. H., Mizushima, N., Packer, M., Schneider, M. D. and Levine, B. (2005). Bcl-2 antiapoptotic proteins inhibit Beclin 1-dependent autophagy. *Cell* **122**, 927-939. doi:10.1016/j.cell.2005.07.002

Pattingre, S., Bauvy, C., Carpentier, S., Levade, T., Levine, B. and Codogno, P. (2009). Role of JNK1-dependent Bcl-2 phosphorylation in ceramide-induced macroautophagy. *J. Biol. Chem.* **284**, 2719-2728. doi:10.1074/jbc.M805920200

Petiot, A., Ogier-denis, E., Blommaart, E. F. C., Meijer, A. J. and Codogno, P. (2000). Distinct classes of phosphatidylinositol 3'-kinases are involved in signaling pathways that control macroautophagy in HT-29 cells. *J. Biol. Chem.* **275**, 992-998. doi:10.1074/jbc.275.2.992

Rabouille, C. (2019). COPII vesicles and the expansion of the phagophore. *Elife* **8**, e44944. doi:10.7554/eLife.44944

Ran, A. F., Hsu, P. D., Wright, J., Agarwala, V., Scott, D. A. and Zhang, F. (2013). Genome engineering using the CRISPR-Cas9 system. *Nat. Protocol.* **8**, 2281-2308. doi:10.1038/nprot.2013.143

Rosciglione, S., Thériault, C., Boily, M.-O., Paquette, M. and Lavoie, C. (2014). Gαs regulates the post-endocytic sorting of G protein-coupled receptors. *Nat. Commun.* **5**, 4556. doi:10.1038/ncomms5556

Sánchez-fernández, G., Cabezudo, S., García-hoz, C., Benincá, C., Aragay, A. M., Mayor, F. and Ribas, C. (2014). Gαq signalling: the new and the old. *Cell. Signal.* **26**, 833-848. doi:10.1016/j.cellsig.2014.01.010

Sharpe, L. J., Luu, W. and Brown, A. J. (2011). Akt phosphorylates Sec24: new clues into the regulation of ER-to-Golgi trafficking. *Traffic* **12**, 19-27. doi:10.1111/j.1600-0854.2010.01133.x

Sondek, J., Lambright, D. G., Noel, J. P., Hamm, H. E. and Sigler, P. B. (1994). GTPase mechanism of Gproteins from the 1.7-Å crystal structure of transducin α-GDP AIF−4. *Nature* **372**, 276-279. doi:10.1038/372276a0

Sullivan, B. M., Harrison-lavoie, K. J., Vladimir, M., Lin, H. Y., Kehrl, J. H., Ausiello, D. A., Brown, D. and Druey, K. M. (2000). RGS4 and RGS2 bind coatomer and inhibit COPI association with golgi membranes and intracellular transport. *Mol. Biol. Cell* **11**, 3155-3168. doi:10.1091/mbc.11.9.3155

Tadevosyan, A., Vaniotis, G., Allen, B. G., Hébert, T. E. and Nattel, S. (2012). G protein-coupled receptor signalling in the cardiac nuclear membrane: evidence and possible roles in physiological and pathophysiological function. *J. Physiol.* **590**, 1313-1330. doi:10.1113/jphysiol.2011.222794

Vaniotis, G., Allen, B. G. and Hébert, T. E. (2011). Nuclear GPCRs in cardiomyocytes : an insider's view of B-adrenergic receptor signaling. *Am. J. Physiol. Heart Circ. Physiol.* **301**, 1754-1764. doi:10.1152/ajpheart.00657.2011

Wang, J., Xie, Y., Wolff, D. W., Abel, P. W. and Tu, Y. (2010). DHHC protein-dependent palmitoylation protects regulator of G-protein signaling 4 from proteasome degradation. *FEBS Lett.* **584**, 4570-4574. doi:10.1016/j.febslet.2010.10.052

Wang, R. C., Wei, Y., An, Z., Zou, Z., Xiao, G., Bhagat, G., White, M., Reichelt, J. and Levine, B. (2012). AKT-mediated regulation of autophagy and tumorigenesis through beclin 1 phosphorylation. *Science* **338**, 956-959. doi:10.1126/science.1225967

Watson, N., Linder, M. E., Druey, K. M., Kehrl, J. H. and Blumer, K. J. (1996). RGS family members: GTPase-activating proteins for heterotrimeric G-protein α-subunits. *Nature* **383**, 172-175. doi:10.1038/383172a0

Wei, Y., Pattingre, S., Sinha, S., Bassik, M. and Levine, B. (2008). Article JNK1-mediated phosphorylation of Bcl-2 regulates starvation-induced autophagy. *Mol. Cell* **30**, 678-688. doi:10.1016/j.molcel.2008.06.001

Weller, S. G., Capitani, M., Cao, H., Micaroni, M., Luini, A., Sallese, M. and McNiven, M. A. (2010). Src kinase regulates the integrity and function of the Golgi apparatus via activation of dynamin 2. *Proc. Natl. Acad. Sci. USA* **107**, 5863-5868. doi:10.1073/pnas.0915123107

Willard, F. S. and Crouch, M. F. (2000). Nuclear and cytoskeletal translocation and localization of heterotrimeric G-proteins. *Immunol. Cell Biol.* **78**, 387-394. doi:10.1046/j.1440-1711.2000.00927.x

Wilson, B. S., Palade, G. E. and Farquhar, M. G. (1993). Endoplasmic reticulum-through-Golgi transport assay based on 0-glycosylation of native glycophorin in permeabilized erythroleukemia cells: role for Gi3. *Proc. Natl. Acad. Sci. USA* **90**, 1681-1685. doi:10.1073/pnas.90.5.1681

Wylie, F., Heimann, K., Le, T. L., Brown, D., Rabnott, G. and Stow, J. L. (1999). GAIP, a Gαi-3-binding protein, is associated with Golgi-derived vesicles and protein trafficking. *Am. J. Physiol.* **276**, 497-506. doi:10.1152/ajpcell.1999.276.2.C497

Yamamoto, K., Ichijo, H. and Korsmeyer, S. J. (1999). BCL-2 is phosphorylated and inactivated by an ASK1/Jun N-terminal protein kinase pathway normally activated at G2/M. *Mol. Cell. Biol.* **19**, 8469-8478. doi:10.1128/MCB.19.12.8469

Zheng, B., Lavoie, C., Tang, T., Ma, P., Meerloo, T., Beas, A. and Farquhar, M. G. (2004). Regulation of epidermal growth factor receptor degradation by heterotrimeric Gαs protein. *Mol. Biol. Cell* **15**, 5538-5550. doi:10.1091/mbc.e04-06-0446

Zhong, Y., Wang, Q. J., Li, X., Yan, Y., Backer, J. M., Chait, B. T., Heintz, N. and Yue, Z. (2009). Distinct regulation of autophagic activity by Atg14L and Rubicon associated with Beclin 1–phosphatidylinositol-3–kinase complex. *Nat. Cell Biol.* **11**, 468-476. doi:10.1038/ncb1854

Zinkel, S., Gross, A. and Yang, E. (2006). BCL2 family in DNA damage and cell cycle control. *Cell Death Differ.* **13**, 1351-1359. doi:10.1038/sj.cdd.4401987